Title: The IRE1α/XBP1 pathway of the unfolded protein response is impaired in pediatric cholestatic liver disease explants

Authors:
Alyssa Kriegermeier[1], Angela Hyon[1], Brian LeCuyer[2], Susan Hubchak[2], Xiaoying Liu[2], Richard M. Green[2]
Alyssa Kriegermeier: akriegermeier@luriechildrens.org
Angela Hyon: ahyon@luriechildrens.org
Brian LeCuyer: brian.lecuyer@northwestern.edu
Susan Hubchak: s-hubchak@northwestern.edu
Xiaoying Liu: xiaoying-liu@northwestern.edu
Richard M. Green: r-green2@northwestern.edu

[1]Department of Pediatrics, Northwestern University, Feinberg School of Medicine, Division of Gastroenterology, Hepatology and Nutrition at Ann & Robert H. Lurie Children's Hospital of Chicago, Chicago, IL 60611

[2]Department of Medicine, Northwestern University, Feinberg School of Medicine, Division of Gastroenterology and Hepatology, Chicago, IL 60611

Contact Information:
Alyssa Kriegermeier, MD
Division of Gastroenterology, Hepatology and Nutrition
Ann & Robert H. Lurie Children's Hospital of Chicago
225 E. Chicago Ave.
Chicago, IL 60611
Phone: 312-503-4385
Fax: 312-227-9645

All authors have no conflict of interest to declare.

Author contributions: AK and RG wrote and edited the manuscript and were responsible for experimental design and oversight. AK and AH performed data analysis. AH, BL, SH and XL performed experiments and contributed to experimental design.

Financial Support:
This work was supported by the Digestive Health Foundation at Northwestern (AK, RG), Pediatric Physician Scientist Research Award (PPSRA) at Ann & Robert H. Lurie Children's Hospital of Chicago (AK), R01 DK121997 (RG), R01 DK093807 (RG), and the Max Goldenberg Foundation Award (RG)

Abstract

Background and Aims: Cholestatic liver diseases (CLD) are the leading indication for pediatric liver transplantation. Bile acids are known to trigger endoplasmic reticulum (ER) stress. The unfolded protein response (UPR) is a coordinated response which functions to decrease ER stress and maintain cellular homeostasis. Dysregulation of the UPR, specifically the inositol-requiring enzyme 1α/X-box protein 1 (IRE1α/XBP1) pathway, has been associated with several adult liver diseases. In this study, we sought to evaluate the UPR in pediatric livers with end-stage CLD and hypothesized there would be altered IRE1α/XBP1 pathway activation compared to normal control livers.

Methods: We evaluated 34 human liver ex-plants which included pediatric CLD, pediatric normal, pediatric non-cholestatic liver disease (autoimmune hepatitis, AIH), adult CLD and adult normal cohorts. We performed RNA sequencing (RNAseq), qPCR and western blotting to identify significantly different pathway activation and assess for changes within the UPR.

Results: Pathway analysis of RNAseq data demonstrated that protein processing in the ER was a significantly differentially expressed pathway in all liver disease cohorts compared to appropriate controls. Pediatric CLD samples had evidence of ongoing ER stress with activation of the PKR-like ER kinase (PERK) pathway but had significantly decreased expression of the IRE1α/XBP1 pathway of the UPR compared to normal controls. Pediatric AIH samples had similar activation of the PERK pathway but notably did not have decreased activation of the IRE1α/XBP1 pathway compared to normal controls.

Conclusion: Pediatric CLD ex-plants have evidence of ongoing ER stress but decreased activation of the protective IRE1α/XBP1 pathway of the UPR. Dysregulation of this pathway may contribute to disease progression and could be a therapeutic target for treating pediatric CLD.

Keywords: cholestasis, liver, ER stress, pediatric

Introduction:

Cholestatic liver diseases (CLD) are the leading indication for pediatric liver transplantation[1]. These include genetic diseases such Alagille syndrome (ALGS), progressive familial intrahepatic cholestasis (PFIC) and others. Though the genetic mutations associated with many of these diseases are now known, a spectrum of severity exists and the underlying factors that influence disease progression are not fully understood. Standard medial therapy for these diverse diseases is supportive care, but treatments altering disease progression that decrease the need for liver factor transplantation are needed.

A major factor responsible for the lack of adequate treatments for pediatric cholestatic liver diseases is the gap in our understanding of the protective hepatic responses to reduce bile acid induced injury in children. Cholestasis and the accumulation of hepatic bile acids increases endoplasmic reticulum (ER) stress in vitro and in animal models[2-5]. ER stress is caused by an excess of unfolded or misfolded proteins and has been shown to be important in the pathogenesis of several liver diseases including NAFLD/NASH, chronic viral hepatitis, and alcohol-related liver diseases[6-9]. The unfolded protein response (UPR) is a protective molecular response present in all eukaryotic cells, that decreases ER stress within cells and restores normal cellular homeostasis. There are 3 pathways of the UPR: the inositol-requiring enzyme 1α/X-box protein 1 (IRE1α/XBP1) pathway, the PKR-like ER kinase (PERK) pathway and the activating transcription factor 6 (ATF6) pathway. In the presence of ER stress, activated phosphorylated IRE1α (pIRE1α) splices XBP1 mRNA to produce the transcriptionally

active spliced form XBP1s. Though primarily protective, if ER stress is prolonged and unresolved, the UPR can trigger apoptosis[10]. Our previous animal studies have demonstrated that UPR pathways regulate liver bile acid synthesis and transporters, and hepatocyte-specific deletion of the UPR protein XBP1 alters bile acid metabolism and susceptibility to liver injury[11-13]. Animal studies demonstrate that developmental changes in UPR activation may be an important factor in hepatic UPR activation and ER stress resolution[14]. However, studies of the hepatic UPR in the pathogenesis of pediatric liver diseases have not been previously performed. Therefore, in this study, we sought to evaluate the hepatic UPR activation in in the livers of pediatric patients with severe cholestatic disease. We hypothesized that there would be inadequate hepatic IRE1α/XBP1 activation in these patients which could be responsible for exacerbated hepatocellular injury and fibrosis. By identifying liver UPR pathways that may be impaired in patients with pediatric cholestatic liver disorders, we could develop novel treatment strategies for a spectrum of pediatric cholestatic liver diseases.

Materials and Methods:

Materials

Antibodies are listed in supplemental table 1. PCR primers were synthesized by either Sigma (St. Louis, MO) or Integrated DNA technologies (Coralville, Iowa), and are listed in supplemental table 2. All other reagents were high grade and purchased from commercial vendors.

Human Samples

A total of 34 human livers were obtained for use in this study at Lurie Children's Hospital (LCH), Chicago, Illinois, and Northwestern University. This study was approved by the LCH institutional review board. Tissues from the biorepositories were collected in accordance with existing IRB regulations at the time of collection. Diseased liver samples including cholestatic liver disease (CLD) and autoimmune hepatitis (AIH) samples were liver explants from patients undergoing liver transplantation. Normal control livers were explants from deceased persons who had donated their liver for liver transplantation but were unable to be utilized for transplantation. Explanted livers were frozen at -80°C. Samples included 7 adult (>18 years of age) normal (aNormal) livers, 9 pediatric (<18 years of age) normal (pNormal) livers, 3 adult CLD livers (aCLD), 10 pediatric CLD livers (pCLD), and 5 pediatric AIH livers. Based on prior known clinical and histopathologic diagnoses, the adult CLD cohort was composed of 2 patients with primary biliary cholangitis (PBC) and 1 patient with primary sclerosing cholangitis (PSC); and the pediatric CLD cohort was composed of 5 patients with Alagille syndrome (ALGS) and 5 patients with progressive familial intrahepatic cholestasis (PFIC).

RNA Extraction, Quantitative Real-time PCR

Total RNA was extracted from frozen liver samples using TRIZOL reagent (Ambion by Life Technologies, Carlsbad, CA), and cDNA was synthesized with the qScript cDNA synthesis kit (Quantabio, Beverly, MD). Quantitative PCR (qPCR) was performed using Power SYBR Green PCR Master Mix (Thermo Fisher Scientific, Waltham, MA) as previously described[12]. Relative expression of the genes of interest were measured by the $\Delta\Delta$Ct method using beta-2 microglobulin (B2M) as reference gene.

RNA sequencing (RNAseq) preparation and analysis

RNA was submitted for all 34 samples (10 pediatric CLD, 3 adult CLD, 5 AIH, 9 pediatric normal, and 7 adult normal). The stranded mRNA-seq was conducted in the Northwestern University NUSeq Core Facility. Briefly, total RNA examples were checked for quality using RINs generated from Agilent Bioanalyzer 2100. RNA quantity was determined with Qubit fluorometer. The Illumina Stranded mRNA Library Preparation Kit was used to prepare sequencing libraries from 100 ng of high-quality RNA samples (RIN>7). All 34 samples met QC standards and were used for the study. The kit procedure was performed without modifications. This procedure includes mRNA purification and fragmentation, cDNA synthesis, 3' end adenylation, Illumina adapter ligation, library PCR amplification and validation. Illumina HiSeq sequencer was used to sequence the libraries with the production of single-end, 50 bp reads at the depth of 20-25 M reads per sample. The quality of reads, in FASTQ format, was evaluated using FastQC. Reads were trimmed to remove Illumina adapters from the 3' ends using cutadapt[15]. Trimmed reads were aligned to the human genome (hg38) using STAR[16]. Read counts for each gene were calculated using htseq-count in conjunction with a gene annotation file for mm10 obtained from Ensembl(http://useast.ensembl.org/index.html)[17]. Normalization and differential expression were calculated using DESeq2 that employs the Wald test[18]. The cutoff for determining significantly differentially expressed genes was an FDR-adjusted p-value less than 0.05 using the Benjamini-Hochberg method[19]. Pathway analysis was performed using Metascape to identify pathways enriched in the significantly differently expressed genes[20]. A maximum of 3000 differentially expressed genes were selected

based on lowest adjusted p values. Heatmaps of the differentially expressed genes were generated in 'R' utilizing results of the DESeq2 analysis.

Western Blotting

Protein homogenates from frozen liver tissue were isolated using T-PER protein extraction reagent (Thermo Scientific) containing protease inhibitor cocktails and Halt phosphatase inhibitors (EMD Millipore, Billerica, MA). Protein quantification was performed using Coomassie Plus protein assay reagent (Thermo Scientific). Equal amounts of protein samples were subjected to immunoblotting for target proteins and immunoreactive bands were visualized using the Amersham ECL western blotting detection kit according to the manufacturer's protocol (GE Healthcare, Piscataway, NJ). Antibodies for GAPDH or Cyclophilin B were used as loading controls.

Tissue Histology Analysis

Sections of frozen liver tissue were thawed overnight in formalin, and histology including H&E and trichrome staining was prepared by the Pathology Core Facility at Robert H. Lurie Comprehensive Cancer Center of Northwestern University. Two blinded investigators (AK, RG) scored trichrome histology slides for degree of fibrosis (F0-F4) based on METAVIR scoring after reviewing 10 fields of view at 10x magnification[21].

Statistics

Data was analyzed using Prism Software and shown as mean ± SEM for all experiments. Comparison between two groups was performed using two-tailed student's t-tests, comparison between 3 or more groups was performed using ANOVA with Tukey's multiple comparisons, and significance was defined as a $p \leq 0.05$.

Results:

Demographic and clinical information

A summary of available demographic/clinical data for the 34 liver samples used in this study is listed in Table 1. The age and sex was available for all normal samples except for 1 pediatric sample. Pediatric normal samples ranged from 22 months – 5 years (mean 3.4 years), and 3/9 were male. The adult normal samples ranged from 19- 66 years (mean 31.6 years) and 2/7 were male. The patient age was available for 2 of 3 aCLD samples (49 and 62 years), and 1 of 3 samples had a sex identified (female). For the pCLD samples, only the liver disease diagnosis was specified, and the age and sex were not routinely identified when collected at this biorepository at LCH. For the AIH samples, age, sex, and laboratory data was available for all samples. The mean AIH patient age was 11.2 years, range (1 – 14 years) and 1/5 AIH samples was male. The average direct bilirubin on the day prior to transplantation for the AIH cohort was 2.36 mg/dL (range <0.2-8.9 mg/dL). Notably, within the AIH cohort, patients 1 and 5 had the only direct bilirubin levels >1mg/dL and these patients were transplanted during their initial disease presentation and met criteria for liver failure (INR>2) during this presentation.

All CLD and AIH liver samples show significant fibrosis

Thirty-two of 34 available samples were graded for fibrosis based on METAVIR scoring by 2 blinded reviewers (AK, RG). The was an insufficient amount of tissue for one pediatric CLD liver sample (with ALGS) and one AIH sample. Based on average METAVIR score, pediatric CLD and AIH samples demonstrated significantly more fibrosis (3.4 $\pm$ 0.2 and 3.9 $\pm$ 0.1 respectively) than pediatric normal samples (0.7 $\pm$ 0.2,

p<0.001), and adult CLD samples had significantly more fibrosis than adult normal samples (4 ± 0 vs 0.6 ± 0.3, p<0.001) (Supp. Fig. 1A, B). When pediatric CLD samples were separated based on disease (ALGS vs PFIC) and compared to AIH and normal samples, all diseases groups had similar fibrosis and all disease groups had significantly more fibrosis than normal controls p<0.001) (Supp. Fig. 1C). This confirmed that all disease cohorts in this analysis are from patients with end-stage liver disease.

RNA-Seq, Principal Component Analysis (PCA), and Pathway analysis of pediatric CLD samples compared to normal controls

Principal component analysis (PCA) of RNAseq data demonstrated that all disease samples (CLD and AIH) cluster distinctly from normal pediatric and normal adult controls (Fig. 1A). Comparing pediatric CLD to normal samples, there were 5,766 significantly differentially expressed genes (adjusted p value <0.05) identified via RNAseq. Metascape pathway analysis demonstrated that genes involving the KEGG pathway hsa04141 *"protein processing in endoplasmic reticulum"* was among the top 5 differentially expressed pathways ($p = 10^{-26}$, Figure 1B). Expression of the specific differentially expressed genes within this pathway demonstrated that expression of most genes was decreased in the pCLD samples compared to pediatric normal controls (Figure 1C). We next performed a sub-analysis of the pediatric CLD cohort and compared PFIC to ALGS samples. RNAseq identified only 351 significantly differentially expressed genes between PFIC and ALGS samples, and when Metascape pathway analysis was performed on these differentially expressed genes, KEGG pathway

hsa04141 “protein processing in endoplasmic reticulum” was not one of the top 100 pathways enriched in these genes, nor were other pathways involved in protein folding (Supp. Fig. 3A).

The hepatic IRE1α/XBP1 pathway of the UPR is decreased in pCLD compared to normal controls

As bile acids are known to trigger ER stress and given the findings from our pathway analysis regarding protein processing in the ER, we sought to identify if there were differences in UPR gene and protein expression between pCLD and normal control samples. We first evaluated the IRE1α/XBP1 pathway. Notably, qPCR demonstrated that compared to normal controls, pCLD samples had a 1.8-fold decrease in IRE1α expression (1.4 ± 0.2 vs 0.8 ± 0.2, $p<0.05$), and a 2.8-fold decrease in XBP1s expression (1.5 ± 0.3 vs 0.5 ± 0.1, $p<0.01$) (Fig. 2A). Additionally, gene expression of the XBP1s downstream targets endoplasmic reticulum DNA J domain-containing protein 4 (ERdj4) and ER degradation enhancing α-mannoside 1 (EDEM1) were also significantly decreased in pCLD samples compared to normal controls (Fig. 2A). EDEM1 was decreased 3.6-fold (1.5 ± 0.2 vs 0.4 ± 0.07, $p<0.001$) and ERdj4 was decreased 2.1-fold (1.0 ± 0.2 vs 0.5 ± 0.07, $p<0.05$). We then compared measured gene expression of liver IRE1α, XBP1s, EDEM1 and ERdj4 expression in PFIC compared to ALGS samples. Though the expression of all 4 genes were lower in PFIC compared to ALGS cohorts, none of these changes were statistically significant (Fig. 3B). Analysis of protein expression demonstrated decreased expression of activated (phosphorylated) IRE1α in pCLD samples compared to normal controls (Fig. 2B). We

then evaluated the PERK and ATF6 pathways of the UPR in our pCLD and normal samples. As phosphorylated (activated) PERK could not be detected on our human western blots, we evaluated for evidence of downstream targets including phosphorylated eukaryotic translation initiation factor 2α eIF2α (p-eIF2α) and activating transcription factor (ATF4). Contrary to our IRE1α/XBP1 pathway findings, there was an increase in protein expression of p-eIF2α and ATF4 in the pCLD (and in both ALGS and PFIC), samples compared to controls suggestive of ongoing ER stress (Fig. 4A, B). Next, ATF6 gene expression was evaluated via qPCR, which demonstrated that there was a trend towards decreased ATF6 expression in pCLD samples compared to controls, but this did not reach statistical significance (1.1 ± 0.2 vs 0.8 ± 0.08, $p=0.08$) (Fig. 4C). Additionally, there was a similar trend but no statistically significant difference in ATF6 gene expression when pediatric normal controls were compared to either ALGS or PFIC cohorts (Supp. Fig. 2).

Pathway analysis and quantitative PCR gene and protein expression of AIH samples compared to normal controls

In order to evaluate if the gene expression findings and UPR changes noted in our pCLD were also in pediatric liver samples from non-cholestatic diseases, we utilized pediatric AIH samples as non-cholestatic disease controls. Utilizing our RNAseq data, we compared pediatric AIH and normal control samples, which identified 3608 differentially expressed genes. Pathway analysis demonstrated that the same KEGG pathway hsa04141 “protein processing in endoplasmic reticulum” was enriched in AIH compared to control samples ($p=10^{-23}$, Fig. 5A). Similar to the pCLD cohort, expression

of the specific genes within this pathway demonstrated that expression was overall decreased in the AIH samples compared to pediatric normal controls (Fig. 5B). However, when we evaluated gene expression within the IRE1α/XBP1 pathway of the UPR compared to normal controls, we identified changes in the AIH cohort that were distinct from the changes we found in our pCLD cohort. We evaluated gene expression of IRE1α, XBP1, EDEM1 and ERdj4 comparing pCLD, pediatric normal and AIH samples via ANOVA. Notably, compared to pCLD, AIH samples had statistically significantly increased expression of IRE1α, XBP1s, and EDEM1 by 4.5-fold, 4.3-fold, and 3-fold ($p<0.001$, $p<0.01$, $p<0.001$ respectively) (Fig. 6A). Of note, ERdj4 gene expression was similar in pCLD and AIH samples (Fig. 6A). Evaluation of the other UPR pathways (PERK and ATF6) in AIH compared to normal controls, demonstrated similar changes to the pCLD cohorts. Specifically, protein expression of p-eIF2α and ATF4 was increased in AIH samples compared to controls suggestive of ongoing ER stress (Fig. 6B), and ATF6 gene expression via qPCR demonstrated that there was no significant difference between AIH and pediatric normal controls (Fig. 6C).

aCLD samples have similar trends in IRE1α/XBP1 pathway expression as pCLD samples compared to normal controls

We next sought to evaluate an adult CLD cohort. Utilizing our RNAseq data to compare aCLD to adult normal controls, there were 4,865 differentially expressed genes. Metascape pathway analysis identified several pathways enriched in these genes, and specifically the KEGG pathway hsa04141 was not one of the top 20 differentially expressed pathways, but it was in the top 100 differentially expressed pathways ($p=10^{-}$

[11] , Fig. 7A). When specifically evaluating gene expression of the IRE1α/XBP1 pathway of the UPR between aCLD and normal samples, this pathway showed a similar trend to the pediatric CLD samples, with decreased gene expression of IRE1α, XBP1s, ERdj4 and EDEM1, however none of these changes reached statistical significance (Fig. 8A). Similar to the pCLD cohort, the aCLD also had decreased protein expression of activated (phosphorylated) IRE1α when compared to normal controls (Fig. 8B). There was also a similar increase in protein expression of p-eIF2α and ATF4 in the aCLD samples compared to controls suggestive of ongoing ER stress, and again no change in expression of ATF6 between aCLD and normal samples (Fig.8 C,D). Finally, we performed Metascape pathway analysis comparing the differentially expressed genes between our pediatric and adult normal samples. There were only 31 significantly differentially expressed genes, and 3 differentially expressed pathways with none involving ER stress or the UPR (Supp. Fig.3).

Conclusion:

Pediatric cholestatic liver diseases are the leading indication for pediatric liver transplantation and there is a lack of effective medical therapies for these diseases that mitigate bile acid induced injury. High concentrations of bile acids are known to trigger ER stress and hepatocellular injury in vitro and in rodents[2-5]. The UPR decreases ER stress and restores cellular homeostasis, and dysregulation of the UPR has been associated with several liver diseases. Notably, adult patients with the cholestatic liver disease PSC who have downregulation of ATF6 expression are at increased risk for more rapid disease progression and clinical complications[22]. Additionally, the

IRE1α/XBP1 pathway has been studied in adult liver disease progression as well as murine models of ER stress. Puri et al demonstrated that decreased production of XBP1s protein was associated with the development of steatohepatitis in adult patients[8]. Additionally, following chemically induced ER stress, liver specific XBP1 knock out (LS-XBP1$^{-/-}$) and XBP1$^{fl/fl}$ mice were shown to have similar activation of the UPR, but LS-XBP1$^{-/-}$ mice have impaired resolution of ER stress with resultant hepatic apoptosis[23]. Recently, our group demonstrated that young mice had decreased XBP1s downstream target activation and were more susceptible to bile acid induced liver injury and apoptosis than adult mice[14]. As there have been no studies evaluating the UPR within pediatric cholestatic liver diseases, in this study we sought to evaluate for evidence of UPR activation or dysregulation in this disease cohort and hypothesized that pediatric cholestatic livers would demonstrate impaired IRE1α/XBP1 pathway activation.

In this study, we showed that pathway analysis comparing pediatric CLD and normal samples identified that the KEGG pathway "*protein processing in endoplasmic reticulum"* was one of the most significantly differentially expressed pathways suggesting the importance of these gene changes. We then demonstrated via qPCR and western blotting that hepatic IRE1α/XBP1 pathway signaling was decreased in pediatric CLD compared to normal liver samples. Our pCLD cohort included patients with clinically diagnosed ALGS and PFIC making the group heterogenous. However, we did not find significant differences between our ALGS and PFIC cohorts related to ER stress and protein processing within our pathway analysis, or in evaluation of the

IRE1α/XBP1 pathway signaling which suggests that one disease group was not solely responsible for these findings. When we evaluated the PERK pathway of the UPR, we found that pCLD samples had evidence of increased pathway activation compared to normal controls. Notably, in the presence of ER stress, p-eIF2α (downstream of PERK) leads to overall decreased protein translation, while selectively allowing translation of certain mRNAs including the transcription factor ATF4[24]. These findings are therefore supportive of ongoing ER stress within the pCLD cohort which one would expect to find. Finally, though there was a trend towards decreased ATF6 expression in the pCLD cohort compared to normal samples, this did not reach statistical significance. Notably, we were unable to evaluate ATF6 protein expression given limitations in our antibody detection of activated ATF6 protein, so we cannot be certain that significant protein changes in ATF6 did not occur in our pCLD cohort. In summary, though PERK pathway activation in the pCLD cohort may be expected given likely ongoing ER stress, these pCLD samples showed no evidence of increased IRE1α/XBP1 pathway activation. This finding is important as dysregulation/decreased activation of the IRE1α/XBP1 pathway in other murine and human liver diseases has been associated with increased liver injury and disease progression.

Next, although pathway analysis of normal compared to AIH samples (which are non-cholestatic explants) also identified significant differences in the "*protein processing within the endoplasmic reticulum"* KEGG pathway, we did not identify decreased expression of the IRE1α/XBP1 pathway within this cohort. In fact, compared to pCLD, the AIH cohort actually had increased expression of IRE1α, XBP1s and EDEM1. The

AIH cohort did demonstrate increased p-eIf2α and ATF4 expression compared controls, similar to the pCLD cohort which again may be seen in the setting of ongoing ER stress.

Finally, in adult CLD samples, similar trends were observed with decreased IRE1α/XBP1 pathway expression and increased PERK pathway expression, however not all changes were statistically significant. Notably, our aCLD was small (n=3), so it may be possible that with additional samples some changes would reach the threshold of statistical significance.

There are several limitations to this study based on the nature of the biorepository we utilized for pCLD, aCLD, pNormal and aNormal samples. Ages of our pCLD were not available, however LCH does not routinely perform liver transplants on patients >18 years of age so we assume these samples are from patients under 18 years of age but cannot confirm this. Additionally, clinical data was not available for any of our CLD samples so we are unable to verify the degree of cholestasis within our pediatric and adult CLD cohorts and cannot verify what clinical criteria were used to make the diagnoses of specific diseases. Through histologic analysis of these cohorts, however, we were able to prove that all disease cohorts (CLD and AIH) had significant fibrosis which supports that these patients had end-stage liver disease at the time of transplant. Another limitation of this study is that all our disease cohorts were liver explants, and we are therefore evaluating for UPR changes at one point in time and cannot comment on whether these changes exacerbated liver injury or are the consequence of it. It is possible that the expression of hepatic UPR pathways in end-stage cholestatic liver

disease may be due to fibrosis, however IRE1α/XBP1 pathway expression differed between pediatric explants from patients with cholestatic compared to autoimmune liver disease. Therefore, it is unlikely that the attenuated activation of the IRE1α/XBP1 pathway noted in our pediatric CLD samples is due to fibrosis alone and rather may be more specific to the cholestatic nature of these diseases.

This study identified that hepatic gene and protein expression of cellular pathways involved in ER stress and the UPR may be important in the pathogenesis of cholestatic liver disease, and specifically that pediatric cholestatic liver disease explants have decreased IRE1α/XBP1 pathway activation compared to normal livers and non-cholestatic disease controls. Since the IRE1α/XBP1 pathway is protective in animal models of cholestasis, and in several human liver diseases, the attenuated expression of this pathway may contribute to disease progression and could therefore be a therapeutic target for treating pediatric cholestatic liver diseases. These data provide new scientific insights and suggest that targeting the UPR, and the IRE1α/XBP1pathway specifically, in these diseases may be a novel therapeutic option.

Figure 1.

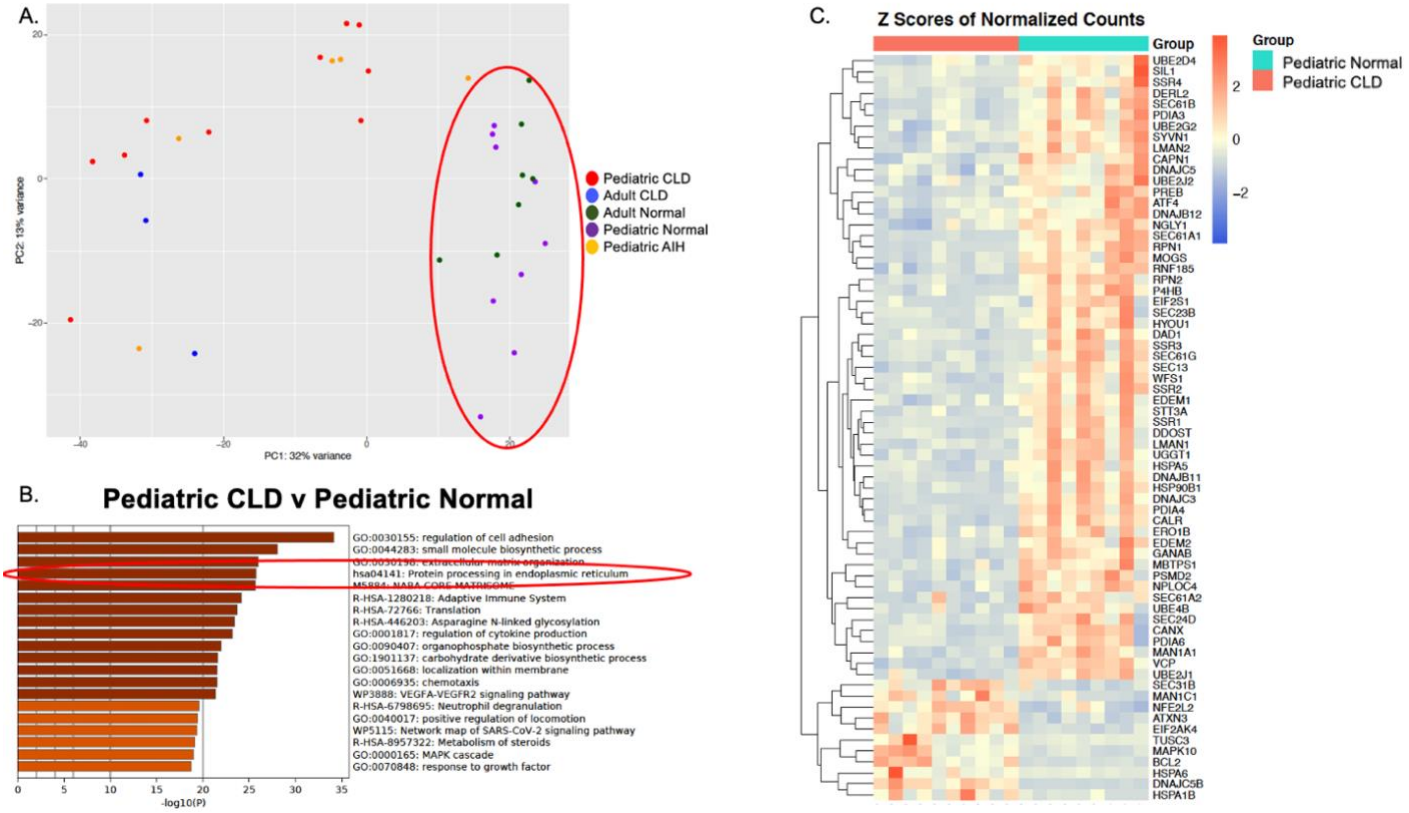

Figure 1. Principal Component Analysis (PCA) and Metascape pathway analysis of pediatric cholestatic liver disease (CLD) samples compared to pediatric normal controls.

A) PCA of RNAseq data demonstrated that all disease samples (CLD and AIH) cluster distinctly from normal pediatric and normal adult controls (circled in red).
B) Metascape pathway analysis of RNAseq differentially expressed genes comparing pediatric cholestatic liver disease (CLD) to normal samples demonstrated that genes involving the KEGG pathway hsa04141 *"protein processing in endoplasmic reticulum"* (circled in red) was among the top 5 differentially expressed pathways ($p = 10^{-26}$).
C) Heatmap demonstrating expression of differentially expressed genes within KEGG pathway hsa04141 between pediatric CLD and normal samples.

Figure 2

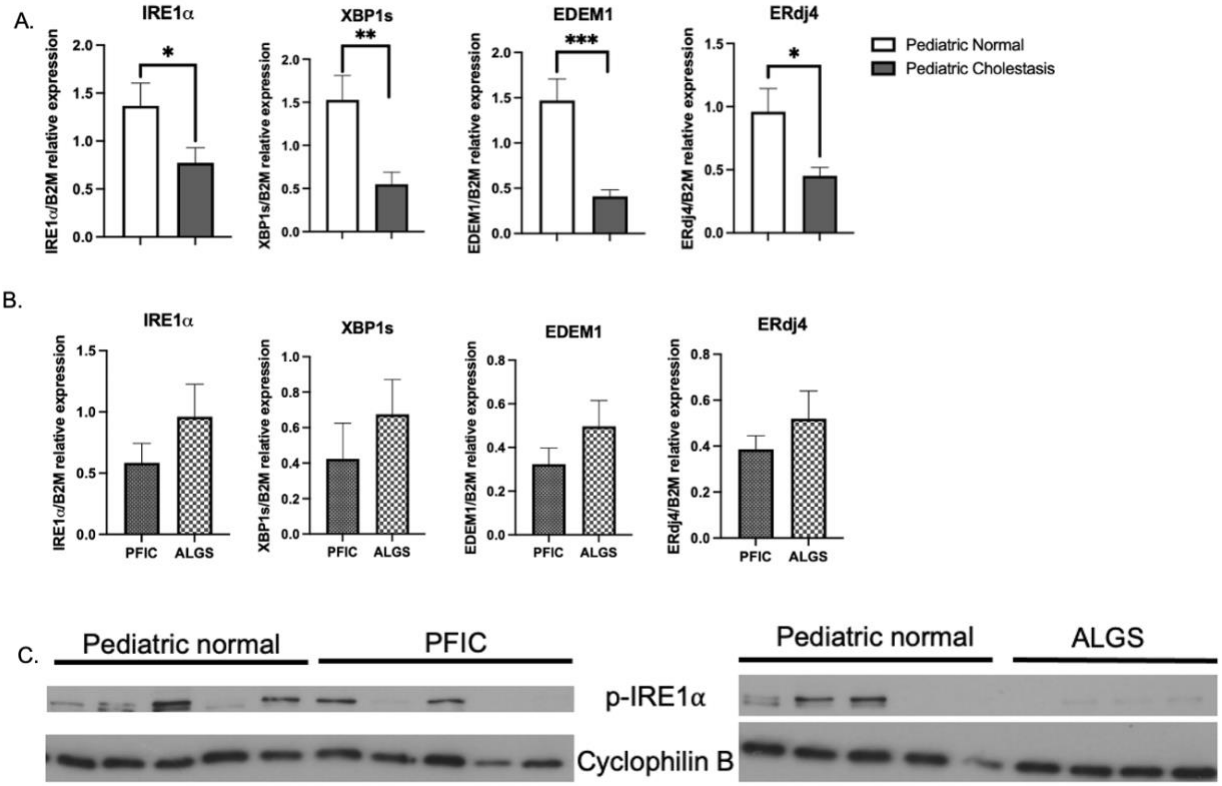

Figure 2. Hepatic IRE1α/XBP1 pathway of the UPR is decreased in pediatric cholestatic liver disease (pCLD) samples compared to pediatric normal controls

A) Hepatic gene expression of IRE1α, XBP1s and downstream targets EDEM1 and ERdj4 were measured via qPCR. Pediatric cholestatic liver samples had a 1.8-fold decrease in IRE1α expression (1.4 ± 0.2 vs 0.8 ± 0.2, *$p<0.05$), a 2.8-fold decrease in XBP1s expression (1.5 ± 0.3 vs 0.5 ± 0.1, **$p<0.01$), a 3.6-fold decrease in EDEM1 expression (1.5 ± 0.2 vs 0.4 ± 0.07, ***$p<0.001$) and a 2.1-fold decrease in ERdj4 expression (1.0 ± 0.2 vs 0.5 ± 0.07, *$p<0.05$).
B) A sub-group analysis of pCLD samples demonstrated no change in hepatic gene expression of IRE1α, XBP1s, EDEM1 and ERdj4 via qPCR when comparing Alagille (ALGS) to progressive familial intrahepatic cholestasis (PFIC) cohorts.
C) Protein expression of activated (phosphorylated) IRE1α (p-IRE1α) was decreased in pCLD (both pediatric PFIC and ALGS) patients compared to normal controls.

Figure 3

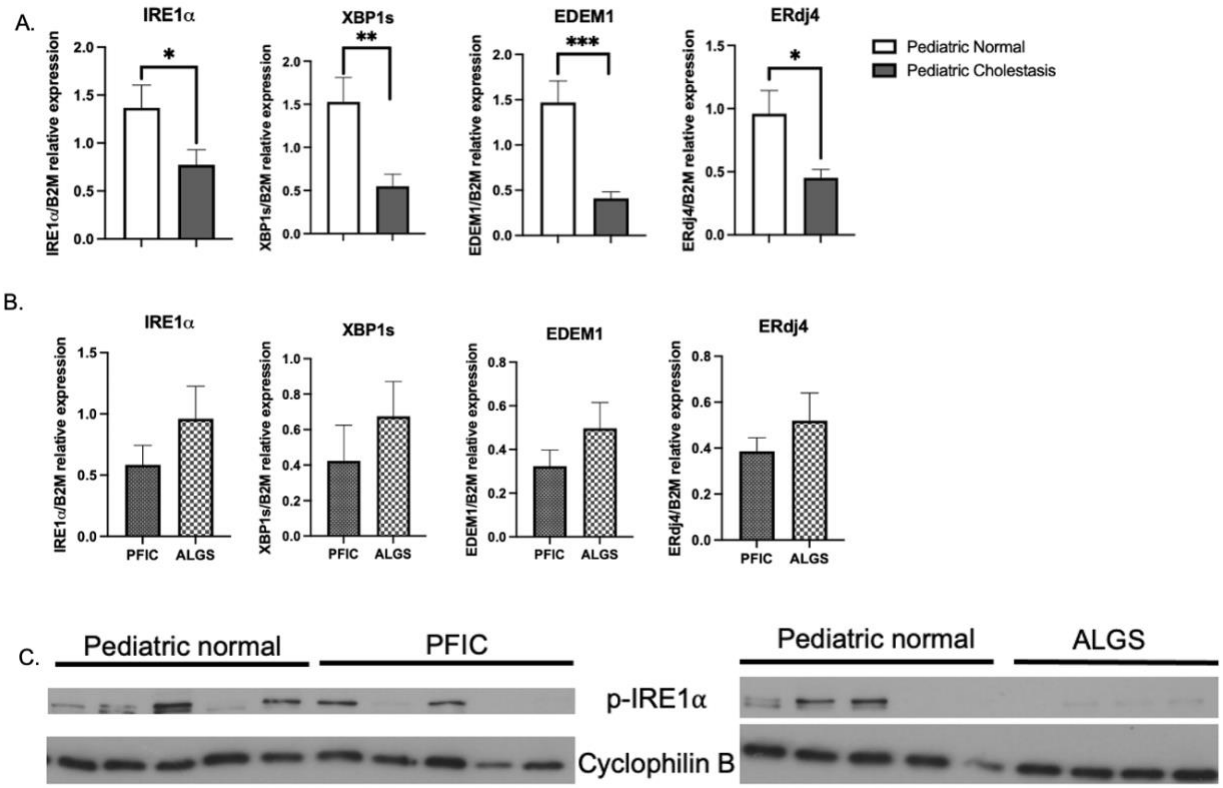

Figure 3. Hepatic protein expression of PERK and ATF6 pathway targets in pediatric cholestatic liver disease (pCLD) samples compared to pediatric normal (pNormal) controls.

A) Western blotting demonstrated an increase in protein expression of phosphorylated (activated) eIF2α (p-eIF2α) and ATF4 in the pCLD samples compared to pNormal controls.
B) Increased p-eIF2α and ATF4 protein expression was found in both Alagille (ALGS) and progressive familial intrahepatic cholestasis (PFIC) samples compared to pediatric normal controls (pNormal).
C) qPCR demonstrated that there was a trend towards decreased ATF6 gene expression in pediatric cholestatic liver samples compared to pediatric normal controls, but this did not reach statistical significance (1.1 ± 0.2 vs 0.8 ± 0.08, $p=0.088$)

Figure 4.

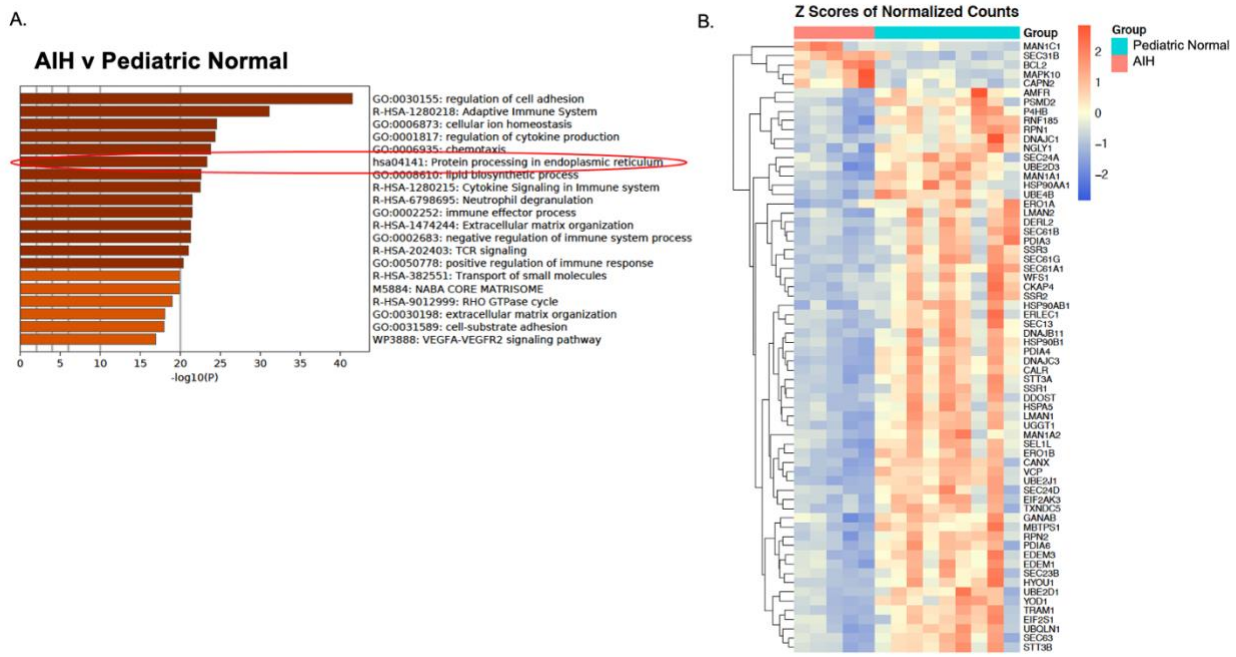

Figure 4. Pathway analysis of pediatric autoimmune hepatitis (AIH) samples compared to pediatric normal controls.

A) Metascape pathway analysis of RNAseq differentially expressed genes comparing AIH to pediatric normal samples demonstrated that genes involving the KEGG pathway hsa04141 *"protein processing in endoplasmic reticulum"* (circled in red) was significantly differentially expressed ($p = 10^{-23}$).
B) Heatmap demonstrating expression of differentially expressed genes within KEGG pathway hsa04141 between AIH and normal samples.

Figure 5.

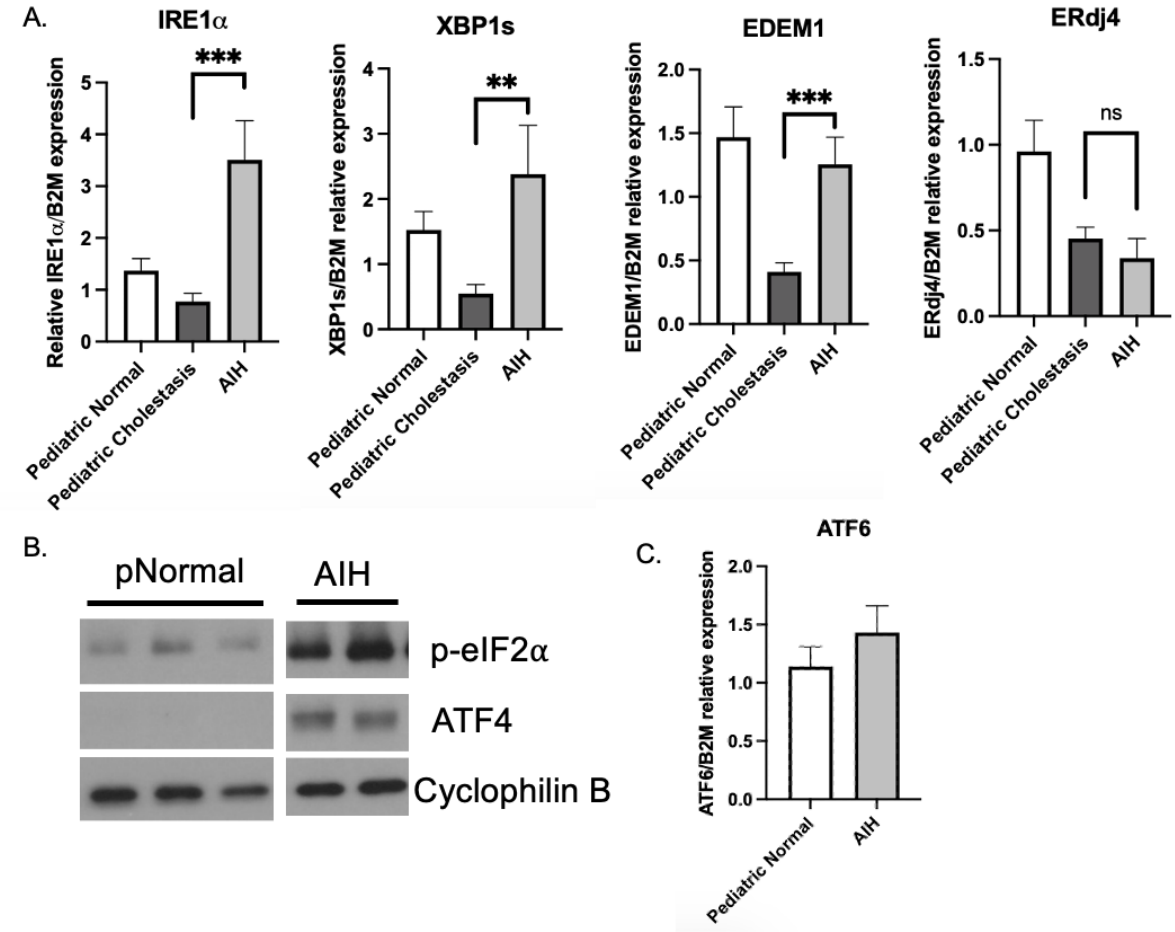

Figure 5. UPR gene and protein expression of autoimmune hepatitis (AIH) samples compared to pediatric normal controls and cholestatic liver disease (pCLD) samples.

A) Via qPCR, compared to pCLD samples, AIH samples had statistically significantly increased expression of IRE1α, XBP1s, and EDEM1 by 4.5-fold, 4.3-fold, and 3-fold (***$p<0.001$, **$p<0.01$, $p<0.001$ respectively) while ERdj4 gene expression was similar.
B) Western blotting demonstrated an increase in protein expression of phosphorylated (activated) eIF2α (p-eIF2α) and ATF4 in the AIH samples compared to pediatric normal controls (pNormal).
C) qPCR demonstrated that there was no significant difference in hepatic ATF6 gene expression between AIH and pediatric normal controls ($p=0.3$)

Figure 6.

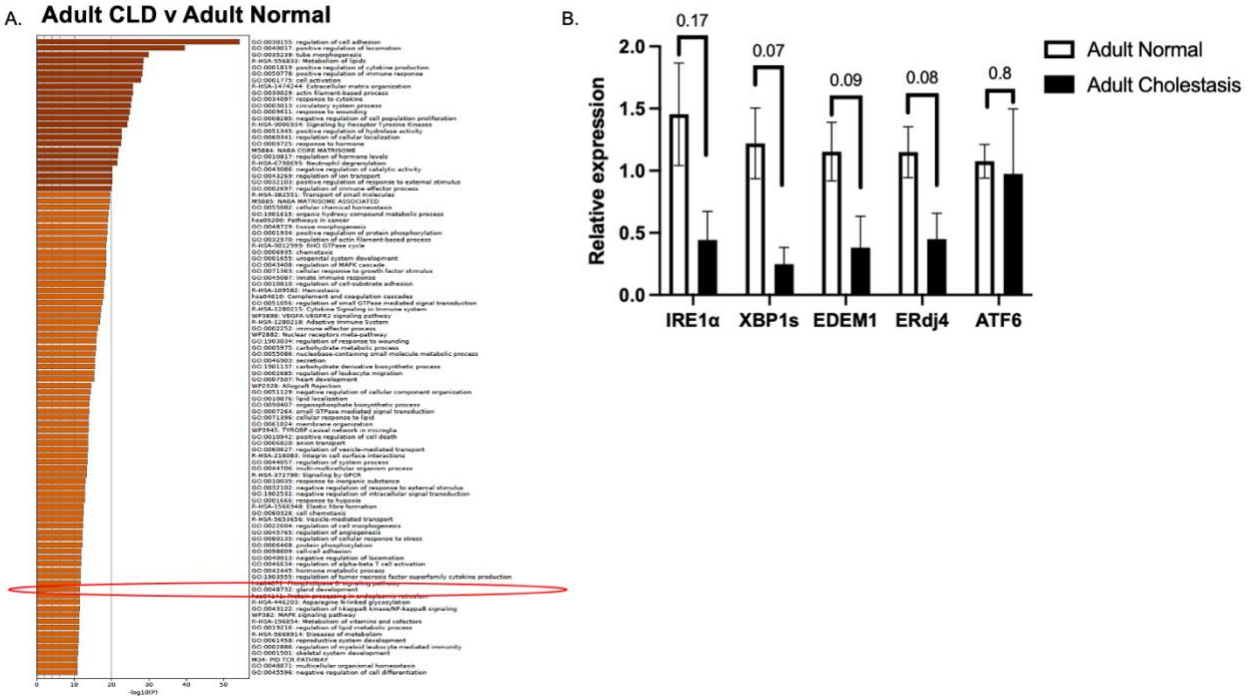

Figure 6. Pathway analysis and IRE1α/XBP1 pathway gene expression of adult cholestatic liver disease (aCLD) samples compared to adult normal controls (aNormal)

A) Metascape pathway analysis of RNAseq differentially expressed genes comparing adult cholestatic liver disease (aCLD) to adult normal samples demonstrated that genes involving the KEGG pathway hsa04141 *"protein processing in endoplasmic reticulum"* (circled in red) was among the top 100 differentially expressed pathways ($p = 10^{-26}$).
B) qPCR demonstrated that there was a trend towards decreased hepatic gene expression of IRE1α, XBP1s, EDEM1 and ERdj4 in adult cholestatic liver samples compared to controls, though none of these changes reached statistical significance. There was no change in hepatic gene expression of ATF6 between adult cholestatic livers and normal controls.

Figure 7.

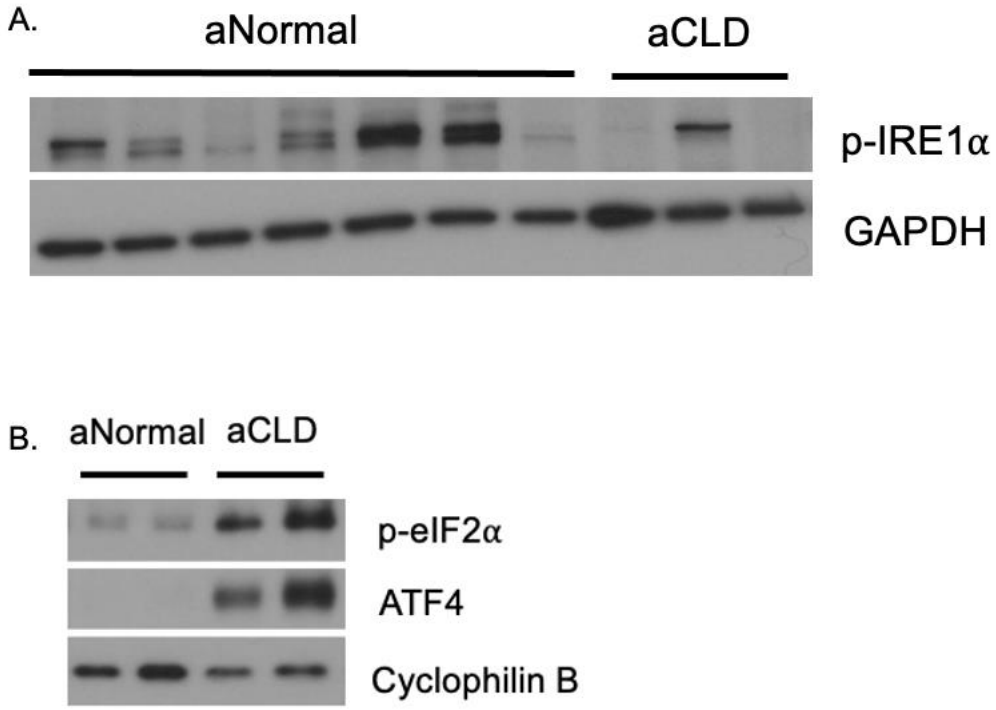

Figure 7. Western blotting of IRE1α and PERK pathway targets in adult cholestatic liver disease (aCLD) samples compared to adult normal controls (aNormal).

A) There was decreased protein expression of activated (phosphorylated) IRE1α in aCLD samples compared to aNormal samples.
B) There was an increase in protein expression of phosphorylated (activated) eIF2α (p-eIF2α) and ATF4 in aCLD samples compared to aNormal controls.

1. Kim WR, Lake JR, Smith JM, et al. OPTN/SRTR 2017 Annual Data Report: Liver. Am J Transplant 2019;19 Suppl 2:184-283.
2. Bernstein H, Payne CM, Bernstein C, et al. Activation of the promoters of genes associated with DNA damage, oxidative stress, ER stress and protein malfolding by the bile salt, deoxycholate. Toxicol Lett 1999;108:37-46.
3. Bochkis IM, Rubins NE, White P, et al. Hepatocyte-specific ablation of Foxa2 alters bile acid homeostasis and results in endoplasmic reticulum stress. Nat Med 2008;14:828-36.
4. Tamaki N, Hatano E, Taura K, et al. CHOP deficiency attenuates cholestasis-induced liver fibrosis by reduction of hepatocyte injury. Am J Physiol Gastrointest Liver Physiol 2008;294:G498-505.
5. Tsuchiya S, Tsuji M, Morio Y, et al. Involvement of endoplasmic reticulum in glycochenodeoxycholic acid-induced apoptosis in rat hepatocytes. Toxicol Lett 2006;166:140-9.
6. Henkel AS, Elias MS, Green RM. Homocysteine supplementation attenuates the unfolded protein response in a murine nutritional model of steatohepatitis. J Biol Chem 2009;284:31807-16.
7. Ji C, Kaplowitz N. Betaine decreases hyperhomocysteinemia, endoplasmic reticulum stress, and liver injury in alcohol-fed mice. Gastroenterology 2003;124:1488-99.
8. Puri P, Mirshahi F, Cheung O, et al. Activation and dysregulation of the unfolded protein response in nonalcoholic fatty liver disease. Gastroenterology 2008;134:568-76.

9. Tardif KD, Mori K, Siddiqui A. Hepatitis C virus subgenomic replicons induce endoplasmic reticulum stress activating an intracellular signaling pathway. J Virol 2002;76:7453-9.

10. Hetz C, Papa FR. The Unfolded Protein Response and Cell Fate Control. Mol Cell 2018;69:169-181.

11. Liu X, Guo GL, Kong B, et al. Farnesoid X receptor signaling activates the hepatic X-box binding protein 1 pathway in vitro and in mice. Hepatology 2018;68:304-316.

12. Liu X, Henkel AS, LeCuyer BE, et al. Hepatic deletion of X-box binding protein 1 impairs bile acid metabolism in mice. J Lipid Res 2017;58:504-511.

13. Henkel AS, LeCuyer B, Olivares S, et al. Endoplasmic Reticulum Stress Regulates Hepatic Bile Acid Metabolism in Mice. Cell Mol Gastroenterol Hepatol 2017;3:261-271.

14. Kriegermeier A, Hyon A, Sommars M, et al. Hepatic X-box binding protein 1 and unfolded protein response is impaired in weanling mice with resultant hepatic injury. Hepatology 2021.

15. Martin M. Cutadapt Removes Adapter Sequences From High-Throughput Sequencing Reads. EMBnet.journal 2011;17:10-12.

16. Dobin A, Davis CA, Schlesinger F, et al. STAR: ultrafast universal RNA-seq aligner. Bioinformatics 2013;29:15-21.

17. Anders S, Pyl PT, Huber W. HTSeq--a Python framework to work with high-throughput sequencing data. Bioinformatics 2015;31:166-9.

18. Love MI, Huber W, Anders S. Moderated estimation of fold change and dispersion for RNA-seq data with DESeq2. Genome Biol 2014;15:550.

19. Haynes W. Benjamini–Hochberg Method. In: Dubitzky W, Wolkenhauer O, Cho K-H, Yokota H, eds. Encyclopedia of Systems Biology. New York, NY: Springer New York, 2013:78-78.

20. Zhou Y, Zhou B, Pache L, et al. Metascape provides a biologist-oriented resource for the analysis of systems-level datasets. Nat Commun 2019;10:1523.

21. Bedossa P, Poynard T. An algorithm for the grading of activity in chronic hepatitis C. The METAVIR Cooperative Study Group. Hepatology 1996;24:289-93.

22. Gindin Y, Chung C, Jiang Z, et al. A Fibrosis-Independent Hepatic Transcriptomic Signature Identifies Novel Drivers of Disease Progression in Primary Sclerosing Cholangitis. Hepatology 2020.

23. Olivares S, Henkel AS. Hepatic Xbp1 Gene Deletion Promotes Endoplasmic Reticulum Stress-induced Liver Injury and Apoptosis. J Biol Chem 2015;290:30142-51.

24. Kaplowitz N, Than TA, Shinohara M, et al. Endoplasmic reticulum stress and liver injury. Semin Liver Dis 2007;27:367-77.